

Exploring Thallium Compounds as Thermoelectric Materials: Seventeen New Thallium Chalcogenides

Michael A. McGuire,[†] Thomas K. Reynolds,^{§,‡} and Francis J. DiSalvo^{*,§}

Department of Physics, Clark Hall, and Department of Chemistry and Chemical Biology,
Baker Laboratory, Cornell University, Ithaca, New York 14853

Received February 23, 2005

We have begun investigating thallium-containing compounds as candidate thermoelectric materials. Alkali metal chalcogenide systems have produced compounds with promising thermoelectric properties, and the chemistry of the Tl⁺ cation is similar to that of the alkali metals. However, Tl is less electropositive and heavier than all alkali metals (except Fr). This may lead to compounds with lower electrical resistivity and lower thermal conductivity, both important for thermoelectric performance. Unlike the alkali metals, Tl⁺ has a lone pair of electrons which can be stereochemically active and can influence coordination geometries. Here we report the results of our initial study of quaternary Tl chalcogenide systems. We present the synthesis and structure of 17 new compounds. Some are isostructural to known alkali metal compounds, and some are new structure types. We discuss the activity of the Tl lone pairs. In addition, we have measured the thermoelectric properties (electrical resistivity, thermal conductivity, and thermopower) and band gaps of some of these materials. All of the measured thermal conductivities are extremely low; however, most of the materials are too resistive for thermoelectric applications, at least as currently prepared.

Introduction

The performance of a thermoelectric material is characterized by the dimensionless figure of merit $ZT = (S^2/\rho\kappa)T$ where S is the thermopower, ρ is the electrical resistivity, κ is the thermal conductivity, and T is the absolute temperature.¹ Hence, thermoelectric (TE) materials researchers seek compounds that have a high thermopower and at the same time are good electrical conductors and poor thermal conductors. Currently, doped alloys based on Bi₂Te₃ are used in most cooling devices and have $ZT \approx 1$ near room temperature.² If $ZT = 4$ can be achieved, the efficiency of TE cooling devices would equal that of compressor-based home refrigerators.³ This could lead to widespread applications for such devices.

One major area of current TE research is the synthesis and characterization of new alkali metal (AM) chalcogenide compounds. AM compounds show a great diversity of structural features including isolated metal-chalcogenide units, 1-D chains, 2-D layers, and 3-D networks.⁴ However, the low electronegativity of AMs can lead to large band gaps and increased scattering of charge carriers. The resulting higher values of resistivity are not optimal for TE applications. The reactivity of AMs also may lead to compounds that are unstable when exposed to air or moisture, adding

considerable complexity to devices that would utilize them. Despite these possible disadvantages, some AM compounds have been discovered which show promising TE properties. In particular the figure of merit of CsBi₄Te₆ exceeds that of optimized Bi₂Te₃ alloys below about 250 K.⁵ We would like to take advantage of the rich chemistry of AMs while avoiding the properties that hinder TE performance. Tl may be an interesting element in this respect since it can behave as a pseudo-AM.

In contrast to other group 13 elements, Tl prefers the +1 oxidation state (although Tl³⁺ is known), and the many similarities between the chemistry of AM and Tl have been noted.⁶ In addition, many Tl analogues of AM solid state compounds are known to exist, especially among the oxides. This leads us to believe that the diversity seen in AM chalcogenide compounds may also exist in Tl-containing systems.

The electronegativity of Tl (2.04) is much higher than that of any AM, which should lead to less ionic compounds with smaller band gaps and thus higher carrier mobility. Thallium is also heavier than any stable AM. Inclusion of heavy atoms is a well-established route toward low thermal conductivity. Finally, compounds containing Tl tend to be less sensitive to air and moisture than AM compounds. Unlike AMs, Tl⁺ has a lone pair of electrons that can be stereoactive and may lead to an even greater diversity of structures. Based on these observations, we believe that investigation of Tl-containing chalcogenides may lead to the discovery of improved TE materials.

* To whom correspondence should be addressed. E-mail: fjd3@cornell.edu.

[†] Department of Physics.

[§] Department of Chemistry and Chemical Biology.

[‡] Current address: Intel Corporation, Hillsboro, OR 97124-6463.

(1) Goldsmid, H. *CRC Handbook of Thermoelectrics*; CRC Press: Boca Raton, FL, 1995.

(2) Yim, W. M.; Rosi, F. D. *Solid-State Electron.* **1972**, *15*, 1121.

(3) DiSalvo, F. J. *Science* **1999**, *285*, 703.

(4) See for example Gutzmann, A.; Näther, C.; Bensch, W. *Acta Crystallogr.* **2004**, *C60*, i11 and references therein.

(5) Chung, D.-Y.; Hogan, T.; Brazis, P.; Rocci-Lane, M.; Kannewurf, C.; Bastea, M.; Uher, C.; Kanatzidis, M. G. *Science* **2000**, *287*, 1024.

(6) Greenwood, N.; Earnshaw, A. *Chemistry of the Elements*; Pergamon Press: Elmsford, NY, 1984.

Quaternary Tl–chalcogenide systems have been little studied. The current version of the Inorganic Crystal Structure Database (ICSD) lists 20 quaternary Tl sulfides, only 3 quaternary Tl selenides, and only 2 quaternary Tl tellurides. Undoubtedly, one reason for the lack of extensive study of these systems to date is the high toxicity of Tl. This can limit the range of applications of Tl-based TE materials. As a reference, we can compare the toxicity of Tl (LD₅₀ = 4.5 mg/kg man) to that of Pb (LD₅₀ = 155 mg/kg man) and Bi (LD₅₀ = 221 mg/kg man), as reported on Material Safety Data Sheets. It is interesting to note that the known mechanism of Tl toxicity is related to its similarity to AMs. Cell membranes cannot distinguish between Tl and potassium, and Tl interferes with vital potassium-dependent processes.⁷ Despite this high toxicity, if a high-performance material is discovered, it may find use in niche applications, and with proper device and safety engineering may be suitable for commercial use. In addition, even if the materials could not be used, they may provide a proof of principle by showing that the goal of $ZT = 4$ in bulk materials is achievable.

The thermoelectric properties of some ternary Tl compounds have already been investigated. The ternary compound Tl₂SnTe₅ (isostructural to K₂SnTe₅ and Cs₂SnTe₅) has a figure of merit at room temperature equal to that of nonoptimized Bi₂Te₃ ($ZT = 0.6$).⁸ Tl₆BiTe₆ was found to have extremely low thermal conductivity and $ZT = 1.2$ at 500 °C.⁹ Above about 300 °C, TlSbTe₂ performs as well as PbTe and the filled skutterudites.¹⁰

We have begun our study of quaternary Tl–chalcogenide systems both by attempting to synthesize analogues of known AM compounds and by investigating phase diagrams such as Tl–M1–M2–X where M1 and M2 are transition or main group metals and X is S, Se, or Te. This has led to the discovery of many new compounds, some analogous to known AM compounds and some adopting new structure types. Our results demonstrate both the similarities and differences between the solid state chemistry of Tl and AMs.

In this paper we present 17 new Tl-containing multinary chalcogenides. The structures are discussed and compared to known AM compounds. In general Tl will be treated as a simple single-electron donor in the description of crystal structures. This means that we will focus on the framework composed of the non-Tl atoms and consider the Tl atoms as filling spaces between structural units (chains and layers). Due to the less ionic nature of Tl, this viewpoint may not be as valid as it is for AMs. So we must keep in mind that this construction is used only to aid in the visualization of the crystal structures, and that there may be significant mixing between Tl and chalcogen orbitals in bands at or near the Fermi level. This mixing should result in less anisotropic physical properties than the views of the crystal structures

shown might suggest. The coordination of Tl in these compounds will be discussed in a separate section.

The outline of the paper is as follows. Results are presented in the following section and include the crystal structure description of all the new compounds, as well as the measured TE properties and band gaps of many. Experimental details and figures showing compounds with known isostructural AM analogues can be found in the Supporting Information. The compounds are presented in two sets. The first set of compounds that will be discussed are either isostructural to, or show significant structural similarities to, known AM compounds. This first set includes Tl₂CeP₂S₇, Tl₃Ti₂P₅S₁₈, Tl₂Cu₂SnS₄, Tl₅AgTi₆Se₂₇, Tl₃CuNb₂Se₁₂, Tl₂Cu₂SnTe₄, Tl₂Ag₂SnTe₄, Tl₃Zr_{1.4}Sn_{1.6}Te₆, TlTiPS₅, Tl₂Au₂Sn₂Se₆, and TlLaGeSe₄. Compounds in the second set do not show structural similarities to any known AM compounds containing the same elements listed in the ICSD. This set includes Tl₂BiP₂S₇, Tl_{1.68}NiTi₂S₅, Tl₂Cu₂P₂Se₆, Tl₂Au₂P₂Se₆, TlInP₂Se₆, and Tl_{11.5}Sb_{11.5}Cu₈Se₂₇. The coordination environments of the Tl atoms in these structures, with emphasis on the activity of the lone pair of electrons on Tl⁺, are then presented and discussed.

Results and Discussion

Compounds Isostructural or Similar to Known AM Compounds. *Tl₂CeP₂S₇*. An attempt was made to synthesize the Tl analogue to the known compound K₃CeP₂S₈.¹¹ No evidence of the target compound was found in the reaction product; however, yellow platelets of the title composition were recovered and proved to be isostructural to K₂LaP₂S₇.¹² This compound is monoclinic ($P2_1/n$) with 2-dimensional (2-D) layers of composition $[\text{Ce}_2(\text{PS}_4)_2(\text{P}_2\text{S}_6)]^{4-}$, which run parallel to the (101) plane. Ce is coordinated by eight S atoms: four from two edge-bonded PS₄ units, one from a corner-bonded PS₄ unit, and three from an S₃P–PS₃ unit (two from an edge-bonded PS₃ subunit and one from the other PS₃ subunit). The Tl atoms reside between these layers, and the composition can be written as Tl₄Ce₂(PS₄)₂(P₂S₆). In this structure Tl(1) is coordinated to 10 sulfur atoms in a distorted bi-capped cubic environment, and Tl(2) is coordinated in an irregular geometry to eight S atoms (vide infra).

Since this compound is yellow, we did not investigate its TE properties.

Tl₃Ti₂P₅S₁₈. This compound is isostructural to the AM compound K₃Ti₂P₅S₁₈,¹³ but was discovered in an attempt to make the Tl analogue of the known compound NaTi₂P₃S₁₂.¹⁴ The compound is monoclinic ($C2/c$) and forms black needles. Chains of composition $[\text{Ti}_2\text{P}_5\text{S}_{18}]^{3-}$ separated by Tl atoms run diagonally in the ac plane. In these chains, Ti is coordinated to six S atoms in a distorted octahedral geometry, and P is tetrahedrally coordinated by S. The TiS₆ octahedra are formed by edge bridging of three tetrahedral PS₄ units

- (7) Galván-Arzate, S.; Santamaría, A. *Toxicol. Lett.* **1998**, 99, 1.
- (8) Sharp, J. W.; Sales, B. C.; Mandrus, D. G.; Chakoumakos, B. C. *Appl. Phys. Lett.* **1999**, 74, 3794.
- (9) Wölfling, B.; Kloc, C.; Teubner, J.; Bucher, E. *Phys. Rev. Lett.* **2001**, 86, 4350.
- (10) Kurosaki, K.; Uneda, H.; Muta, H.; Yamanaka, S. *J. Alloys Compd.* **2004**, 376, 43.

- (11) Gauthier, G.; Jobic, S.; Brec, R.; Rouxel, J. *Inorg. Chem.* **1998**, 37, 2332.
- (12) Evenson, C.; Dorhout, P. *Inorg. Chem.* **2001**, 40, 2884.
- (13) Derstroff, V.; Tremel, W.; Regelsky, G.; Schmedt auf der Günne, J.; Eckert, H. *Solid State Sci.* **2002**, 4, 731.
- (14) Cieren, X.; Angenault, J.; Couturier, J.-C.; Jaulmes, S.; Querton, M.; Robert, F. *J. Solid State Chem.* **1996**, 121, 230.

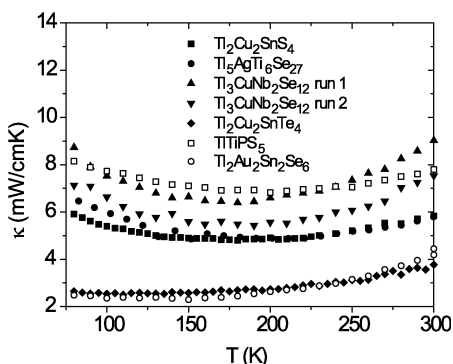


Figure 1. The measured thermal conductivities of six of the compounds reported in this work.

to each Ti. These tetrahedra then either corner share with other PS_4 tetrahedra or edge share with distorted Ce-centered octahedra to form the chains. Tl(2) is disordered over two sites, each half occupied. This disorder is not seen in the AM compound. Both Tl(1) and Tl(2) are again irregularly coordinated by eight S atoms in one-sided environments which could accommodate lone pairs (*vide infra*).

Attempts to make this compound in bulk gave a mixture of the target phase and a minor ($\sim 10\%$) unidentified impurity phase.

$\text{Tl}_2\text{Cu}_2\text{SnS}_4$. Elements were loaded in a 2:2:1:4 ratio in an attempt to make the Tl analogue of the known compound $\text{Rb}_2\text{Cu}_2\text{SnS}_4$.¹⁵ The reaction product contained black block-like crystals of $\text{Tl}_2\text{Cu}_2\text{SnS}_4$, which is isostructural to the AM compound. The structure is orthorhombic, space group *Ibam*, and is made up of $[\text{Cu}_2\text{SnS}_4]^{2-}$ layers separated by Tl. The layers are formed by chains made up of edge-sharing CuS_4 tetrahedra running parallel to the *a* axis and joined by Sn atoms forming SnS_4 tetrahedra. Between the layers Tl has slightly distorted cubic coordination by S (*vide infra*).

The thermal conductivity of a polycrystalline pellet of this material was measured. Figure 1 shows the thermal conductivity of this compound, and of the other compounds which were measured. The thermal conductivity of $\text{Tl}_2\text{Cu}_2\text{SnS}_4$ is very low, less than half that of optimized Bi_2Te_3 alloys at room temperature.² High sample and/or contact resistance prevented the measurement of resistivity and thermopower.

$\text{Tl}_5\text{AgTi}_6\text{Se}_{27}$. This compound was discovered in a successful attempt to synthesize the Tl analogue to the known compounds $\text{Cs}_5\text{AgTi}_6\text{Se}_{27}$ and $\text{Rb}_5\text{AgTi}_6\text{Se}_{27}$.¹⁶ Black needles were recovered from the reaction product and were determined to have the target composition. The AM analogues also form as black needles. As in many AM compounds, these are properly Zintl phases where the octet rule is satisfied by forming direct Se–Se single bonds. The structure is trigonal (space group $P3_1c$). Ti is in an irregular seven-coordinate environment, bonded to Se. The Ti polyhedra face share in pairs, and these pairs then share trans-edges to form 1-D chains along the hexagonal *c*-axis. The Ag ions reside between these chains and are in octahedral coordination by Se. The Ag-centered octahedra join three chains of Ti-centered polyhedra together in isolated groups. Tl(1) is

irregularly coordinated by six Se atoms. Tl(2) is coordinated by nine Se atoms in a distorted tri-capped trigonal prism. Tl(3) is coordinated to nine Se atoms in a symmetrical, but one-sided, environment (*vide infra*).

The Se–Se dimers have a formal charge of -2 and the structural formula can be written $\text{Tl}_5\text{AgTi}_6(\text{Se}_2)_{12}\text{Se}_3$. The formal charge on Ti is $+4$, while Ag and Tl are both $+1$. Ti has an irregular coordination, bonded to four Se–Se dimers and one Se^{2-} anion. The Ti atom is bonded to both Se atoms of two of the dimers, but only one Se atom of the other two dimers. The distances between the pairs of Se atoms vary from 2.35 Å to 2.37 Å. The Se–Se bond distance in elemental Se is about 2.4 Å.¹⁷ All other Se–Se distances in this structure are greater than 3.0 Å. This coordination of Ti by Se is unusual since Ti is often nearly octahedrally coordinated by six Se anions.

A polycrystalline pellet of $\text{Tl}_5\text{AgTi}_6\text{Se}_{27}$ was made for thermoelectric properties measurements. Figure 1 shows the measured thermal conductivity of this sample. The thermal conductivity is very low, less than half that of optimized Bi_2Te_3 alloys at room temperature. At 300 K the thermopower was measured to be $-820 \mu\text{V/K}$, indicating n-type conduction. The measured resistivity at 300 K was $1.2 \times 10^4 \Omega\text{cm}$. This is too large for TE applications, but is an order of magnitude lower than $\text{Cs}_5\text{AgTi}_6\text{Se}_{27}$, which has a resistivity at room temperature of $2.5 \times 10^5 \Omega\text{cm}$.¹⁶

$\text{Tl}_3\text{CuNb}_2\text{Se}_{12}$. This compound was made in a successful attempt to synthesize the Tl analogue of the known compound $\text{K}_3\text{CuNb}_2\text{Se}_{12}$.¹⁸ This compound crystallizes in the monoclinic space group $P2_1/n$ as black needles, the same color as the AM analogue. In this structure the Nb atoms are coordinated to seven Se atoms in a distorted pentagonal bipyramid. These polyhedra are paired by face sharing and each member of the pair edge shares with a CuSe_4 tetrahedron forming chains running perpendicular to the *b* axis. Tl atoms reside between these chains. In this structure, Tl(1) has irregular 7-fold coordination and Tl(2) irregular 8-fold coordination by Se. Tl(3) is in a distorted mono-capped cubic environment, coordinated by nine Se atoms (*vide infra*).

There is a substantial amount of Se–Se bonding in this structure. In each CuSe_4 unit, two of the Se atoms are bonded to the same Se atom outside the chain forming Se trimers. There is also Se–Se bonding within the chains. Around each Nb four of the five Se atoms that make up the distorted pentagon are bonded, forming two dimers. Dimers are also formed by Se atoms coordinated to neighboring Nb-centered polyhedra. The interatomic distances between paired Se atoms range from 2.36 Å to 2.47 Å. The next closest Se–Se contact is 2.81 Å, which is shorter than the typical Se–Se van der Waals contact of 3.80 Å,¹⁹ but we do not consider it to be a single bond. With these assignments, the composition can be written as $\text{Tl}_3\text{CuNb}_2(\text{Se}_3)(\text{Se}_2)_3\text{Se}_3$. Counting each Se dimer and trimer as -2 , and assigning $+1$ to both Tl and Cu, gives a formal charge of $+5$ for Nb.

The results of TE properties measurements on a polycrystalline pellet of this material are presented in Figures 1 and

(15) Laio, J.-H.; Kanatzidis, M. *Chem. Mater.* **1993**, *5*, 1561.

(16) Huang, F.; Ibers, J. *Inorg. Chem.* **2001**, *40*, 865.

(17) Cherin, P.; Unger, P. *Inorg. Chem.* **1967**, *6*, 1589.

(18) Lu, Y.-J.; Ibers, J. *Inorg. Chem.* **1991**, *30*, 3317.

(19) Bondi, A. *J. Phys. Chem.* **1964**, *68*, 441.

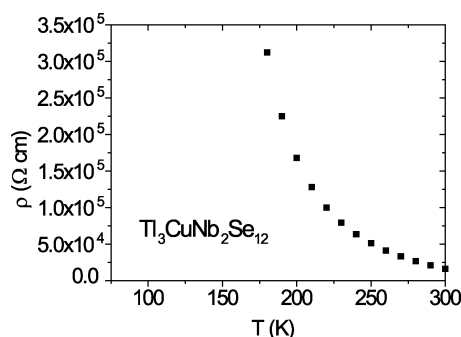


Figure 2. The measured resistivity of $\text{Tl}_3\text{CuNb}_2\text{Se}_{12}$.

2. This compound shows p-type semiconducting behavior, with high resistivity. The thermopower could only be measured near room temperature due to the increasing resistance as T decreased. The measured value at 300 K was $+770 \mu\text{V/K}$, indicating p-type conduction. The thermal conductivity was measured twice, with the sample being removed from the measurement apparatus and then later remounted. The measurements show acceptable reproducibility and low thermal conductivity.

$\text{Tl}_2\text{Cu}_2\text{SnTe}_4$ and $\text{Tl}_2\text{Ag}_2\text{SnTe}_4$. These compounds were discovered in attempts to make Tl analogues of the known compound $\text{K}_2\text{Ag}_2\text{SnTe}_4$.²⁰ $\text{Tl}_2\text{Ag}_2\text{SnTe}_4$ is isostructural to the AM compound. $\text{Tl}_2\text{Cu}_2\text{SnTe}_4$ is not; however, it is very similar. Both Tl compounds form blocklike black crystals, as does $\text{K}_2\text{Ag}_2\text{SnTe}_4$. All three compounds are tetragonal ($I\bar{4}2m$) and have channels running along the c -axis in which Tl atoms reside. The Tl atoms are in a distorted square antiprismatic environment, coordinated by Te atoms. The framework surrounding these channels is different in each case and is made up of Sn and Cu/Ag atoms in tetrahedral coordination.

In these compounds the Sn atom is at the corners (and center) of the unit cell and is tetrahedrally coordinated by Te. The differences among the structures are due to the different sites and occupancies of the Cu or Ag atoms. In $\text{Tl}_2\text{Ag}_2\text{SnTe}_4$ there are two sites partially occupied by Ag. One is at $(0,0,1/2)$ and has occupancy 0.29. The other is displaced from this high-symmetry position to (x,y,z) and thus forms eight equivalent sites around the first Ag atom. These sites have occupancy 0.22 and large displacement ellipsoids, suggesting perhaps further positional disorder. In $\text{Tl}_2\text{Cu}_2\text{SnTe}_4$ the site at $(0,0,1/2)$ is vacant and only the 4-fold site (x,x,z) is occupied by Cu. The occupancy of this site is 0.5. In all of these compounds the tetrahedrally coordinated metal atoms form chains along the c axis. The metal atoms which are offset from high-symmetry positions form bonds to Te atoms coordinated to symmetry-equivalent metal atoms in neighboring chains. This interchain bonding makes the non-Tl-containing part of the structure three-dimensional. The Tl atoms in these structures are found in distorted square antiprisms (vide infra) between the chains.

These compounds have the structural features desired for good thermoelectric materials. A three-dimensional covalent network is present which could provide for good electrical

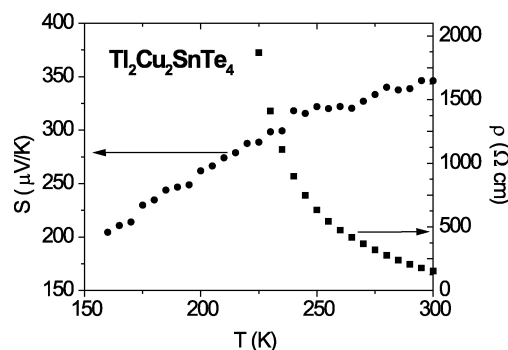


Figure 3. The measured thermopower (circles) and resistivity (squares) of $\text{Tl}_2\text{Cu}_2\text{SnTe}_4$.

transport properties, while the Tl atoms in open channels may act as “rattlers” to scatter heat-carrying phonons to keep the lattice thermal conductivity low.

Attempts to make $\text{Tl}_2\text{Ag}_2\text{SnTe}_4$ in bulk resulted in the target compound as the majority phase along with SnTe and other unidentified phases. However, the Cu analogue was made as a single-phase powder and the results of properties measurements on a polycrystalline pellet are presented in Figures 1 and 3. This p-type semiconducting compound has extremely low thermal conductivity, and a moderate thermopower. However, the resistivity of this material is too high to be useful for thermoelectric applications, unless the carrier density can be increased by suitable doping. The very low thermal conductivity of this compound could be partially due to the disordered Cu atoms.

$\text{Tl}_3\text{Zr}_{1.4}\text{Sn}_{1.6}\text{Te}_6$. This compound was discovered during an investigation of the Tl–Zr–Sn–Te phase diagram. It forms black needles, crystallizes in the rhombohedral space group $R\bar{3}m$, and is isostructural to NaInSe_2 .²¹ The structure consists of sheets of edge-sharing octahedra with Te atoms at the vertices. The centers of the octahedra are randomly occupied by Zr and Sn. The sheets are separated by Tl which has distorted octahedral coordination by Te atoms in the sheets (vide infra). Charge balance is achieved if the Zr/Sn site is split equally and Sn has a charge of +2. Single-crystal X-ray data refinement of the occupancy of this site, requiring the total occupancy to be unity, results in 46% Zr and 54% Sn. This is consistent with the results from standardless energy dispersive electron microprobe analysis of several single crystals which gave an average Zr/Sn ratio of 0.8. This compound is also isostructural to the compound TlSbTe_2 which has shown interesting thermoelectric properties.¹⁰

Attempts to synthesize this compound in bulk have resulted in a multiphase mixture containing the target compound as the majority phase ($\sim 90\%$) and Tl_4SnTe_3 .

TlTiPS_5 . An attempt was made to synthesize the Tl analogue of the known quaternary compounds RbTiPS_5 and KTiPS_5 .²² The reaction product contained black needles of the composition TlTiPS_5 . The Tl and K compounds are not isostructural (TlTiPS_5 is triclinic ($P\bar{1}$) whereas the AM compounds are monoclinic); however, they have very similar structural features. The crystal structure of TlTiPS_5 is shown in Figure 4.

(20) Li, J.; Guo, H.-H.; Proserpio, D. M.; Sironi, A. *J. Solid State Chem.* **1995**, *117*, 247.

(21) Hoppe, R.; Lidecke, W.; Frorath, F. C. *Z. Anorg. Allg. Chem.* **1961**, *309*, 49.

(22) Do, J.; Lee, K.; Yun, H. *J. Solid State Chem.* **1996**, *125*, 30.

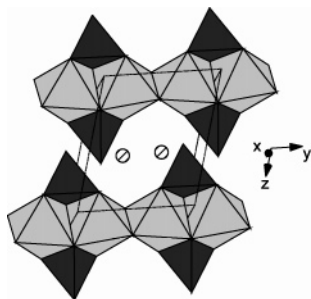


Figure 4. A view of the crystal structure of TlTiPS_5 showing PS_4 tetrahedra (dark) and Ti-centered octahedra (light). Striped circles represent Tl.

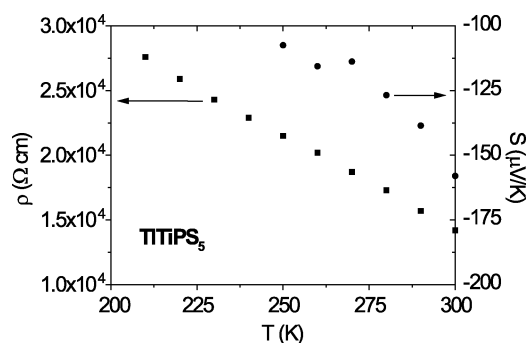


Figure 5. The measured thermopower (circles) and electrical resistivity (squares) of TlTiPS_5 .

Infinite 1-D chains of composition $[\text{TiPS}_5]^-$ run along the b -axis. Ti is coordinated to S in a distorted octahedral geometry, and P is tetrahedrally coordinated to S. The octahedra share edges to form the chains. The P atom is bonded to three S atoms in the chain (at the juncture of two edge-sharing octahedra) and to one S atom outside the chain. In the AM compounds these same chains are seen. However, in these compounds the chains are not staggered along the direction of the chains as they are in the Tl compound (see Figure 4). The staggering of the chains seen in the Tl compound results in the lowering of the crystal symmetry from monoclinic to triclinic. The staggering also results in a less symmetrical environment for the Tl ion than is seen for K and Rb. This could be due to the influence of the Tl lone pair (vide infra).

A polycrystalline pellet of this material was used for thermoelectric properties measurements and the results are shown in Figures 1 and 5. This compound is an n-type semiconductor with high resistivity and relatively low thermal conductivity.

$\text{Tl}_2\text{Au}_2\text{Sn}_2\text{Se}_6$. This compound was discovered in an attempt to make the Tl analogue of $\text{K}_2\text{Au}_2\text{Sn}_2\text{Se}_6$.²³ Black platelike crystals of composition $\text{Tl}_2\text{Au}_2\text{Sn}_2\text{Se}_6$ were recovered from the reaction product. The AM compound was reported to crystallize in the space group $P4/mcc$ with unit cell axes $a = 8.251 \text{ \AA}$ and $c = 19.961 \text{ \AA}$. The strong X-ray diffraction peaks could be indexed with a similar unit cell ($a_0 = 8.097 \text{ \AA}$, $c_0 = 20.069 \text{ \AA}$) and systematic absences suggested the same space group $P4/mcc$. However, weak supercell reflections (on the order of 1–2% of the strongest reflections) clearly indicated a larger unit cell with $a = 11.451 \text{ \AA}$ ($=a_0\sqrt{2}$) and $c = 20.071 \text{ \AA}$.

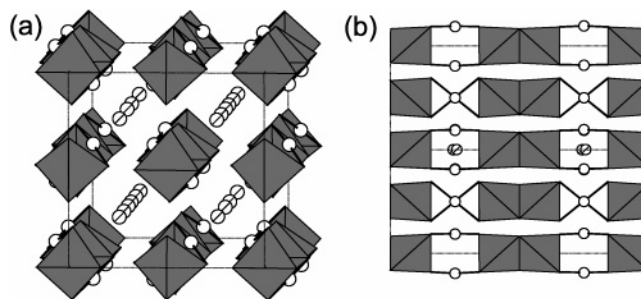


Figure 6. (a) The crystal structure of $\text{Tl}_2\text{Au}_2\text{Sn}_2\text{Se}_6$ viewed nearly down the c -axis, showing Sn-centered tetrahedra, Tl atoms (striped), and Au atoms (white). (b) A view down the $[110]$ axis, showing the displacement of the Tl(4) atoms. In this view Tl1–Tl3 are eclipsed by the Sn_2Se_6 units.

The data were integrated using the $11.451 \text{ \AA} \times 20.071 \text{ \AA}$ unit cell and the reflections sorted based on whether they are allowed by the a_0 , c_0 subcell. The results are summarized in the Supporting Information and clearly indicate that the data are inconsistent with the subcell.

We proceeded to solve the structure in the $11.451 \text{ \AA} \times 20.071 \text{ \AA}$ unit cell. Systematic absences suggested only the space group $P4/ncc$. The crystal structure is shown in Figure 6. It is made up of chains along the c -axis. The chains have composition $[\text{Au}_2\text{Sn}_2\text{Se}_6]^{2-}$ and contain pairs of edge-sharing SnSe_4 tetrahedra linked by Au in linear coordination. The Tl atoms are between these chains. One Tl atom is split between two sites, Tl(2) and Tl(3), which are 2.6 \AA apart.

One K atom in $\text{K}_2\text{Au}_2\text{Sn}_2\text{Se}_6$ was reported to have large displacement parameters, elongated along the c -axis.²³ The authors stated that this may indicate positional disorder. The same large displacement ellipsoids were seen for the equivalent Tl atom when the structure was solved in the smaller unit cell. However, in the larger unit cell, this site corresponds to two sites in different positions, each displaced slightly with respect to the subcell structure (Figure 6). In the larger cell, these two Tl atoms then have nearly spherical displacement ellipsoids. This small displacement is the primary difference between the structures solved in the different unit cells. Due to the weakness of the supercell reflections observed for this compound, and the smaller scattering power of K with respect to Tl, we believe that the supercell may have been overlooked in $\text{K}_2\text{Au}_2\text{Sn}_2\text{Se}_6$.

This material was made into a single-phase polycrystalline pellet for TE properties measurements. Resistivity and thermopower could not be measured due to poor electrical contacts; however, thermal conductivity was measured and is presented in Figure 1. This compound has extremely low thermal conductivity, especially at low temperatures, similar to $\text{Tl}_2\text{Cu}_2\text{SnTe}_4$ presented above.

TlLaGeSe_4 . An attempt was made to synthesize the Tl analogue of the known compound KLaGeSe_4 .²⁴ The reaction product contained a large number of red needle-shaped crystals of the title compound. This compound is orthorhombic ($Pbca$). The structure is shown in Figure 7. It is not isostructural to the AM compound but the two share some structural similarities. The structure is made up of two-dimensional layers perpendicular to the c -axis. LaSe_8 polyhedra share edges to form the layers. The Ge atoms are

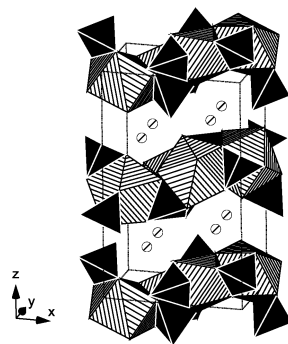


Figure 7. A view of the crystal structure of TlLaGeSe_4 , showing GeSe_4 tetrahedra (black), La-centered polyhedra (striped), and Tl atoms (striped circles).

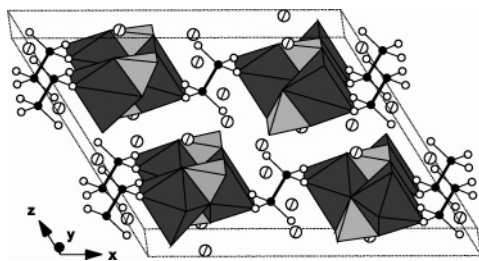


Figure 8. A view of the crystal structure of $\text{Tl}_2\text{BiP}_2\text{S}_7$ showing PS_4 tetrahedra (light), Bi-centered polyhedra (dark), P atoms (black), S atoms (white), and Tl atoms (striped).

positioned between the La-centered polyhedra and are bonded to four Se atoms in tetrahedral coordination. These are typical coordination environments for both La and Ge in chalcogenide compounds. The Tl atoms are located between the layers and again have irregular 6-fold coordination (vide infra). KLaGeSe_4 contains sheets made up of the same building blocks seen in TlLaGeSe_4 ; however, the sheets do not show the corrugation that is seen in the Tl compound.

Since this compound is red, we did not investigate its thermoelectric properties.

Compounds without Known AM Analogues. $\text{Tl}_2\text{BiP}_2\text{S}_7$. Elements were combined in a 1:1:2:7 ratio in an attempt to make the Tl analogue of a known AM compound KBiP_2S_7 .²⁵ The reaction product contained red plates that were determined to be $\text{Tl}_2\text{BiP}_2\text{S}_7$, a compound with no known AM analogue. $\text{Tl}_2\text{BiP}_2\text{S}_7$ crystallizes in the monoclinic space group $C2/c$. Figure 8 shows the crystal structure of this compound. The structure is made up of layers in the ab plane of composition $[\text{Bi}_2(\text{PS}_4)_2(\text{P}_2\text{S}_6)]^{4-}$ separated by Tl atoms. Tl(1) has irregular 9-fold coordination. Tl(2) has six coordinating S atoms with a hemispherical distribution indicative of a stereoactive lone pair (vide infra). Within the layers PS_4 tetrahedra and $\text{S}_3\text{P}-\text{PS}_3$ units bond to Bi atoms. As a result, the Bi atoms are coordinated to seven S atoms. Since $\text{Tl}_2\text{BiP}_2\text{S}_7$ is red, we did not investigate its TE properties.

$\text{Tl}_{1.68}\text{NiTi}_2\text{S}_5$. This compound was discovered during an investigation of the Tl–Ni–Ti–S phase diagram in a reaction with a loading of 2:1:3:7. It crystallizes in the orthorhombic space group $Pnma$ and forms black needlelike crystals with a gold sheen similar to that of TiS_2 . This compound has no known AM analogue. In fact there are no known AM compounds containing Ni, Ti, and S. The crystal

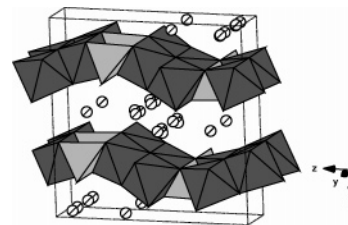


Figure 9. The crystal structure of $\text{Tl}_{1.68}\text{NiTi}_2\text{S}_5$ showing Ti-centered distorted octahedra (dark), Ni-centered tetrahedra (light), and Tl atoms (striped).

structure is presented in Figure 9. In this compound Ni atoms are found in tetrahedral NiS_4 units. Ti is coordinated to S to form distorted octahedra. The octahedra share edges to form 1-D chains along the b axis. The chains are linked by corner sharing in the c direction to form 2-D sheets. Ni atoms also bridge the chains to form the NiS_4 tetrahedra. Tl atoms reside between the layers. There are three crystallographically distinct Tl atoms. Tl(1) is in a distorted, hemispherical, seven-coordinate environment, suggestive of an active Tl lone pair. Tl(2) and Tl(3) are two closely spaced sites which are partially occupied and give the noninteger Tl stoichiometry. These sites are six-coordinate and are near the center of a slightly distorted trigonal antiprism (vide infra).

The fact that the electron count does not readily balance suggests metallic properties which would be consistent with the metallic sheen of the crystals. There are other examples of noninteger stoichiometries in known thallium titanium chalcogenides. For instance, the Tl sites are partially occupied in $\text{Tl}_{0.97}\text{Ti}_5\text{S}_8$ and $\text{Tl}_{0.76}\text{Ti}_6\text{Se}_8$.²⁶

Attempts to prepare this compound as a single-phase bulk sample produced a poorly crystalline mixture containing the target compound, sulfur, and other unidentified phases.

$\text{Tl}_2\text{Cu}_2\text{P}_2\text{Se}_6$. Elements were combined in a 1:1:2:5 ratio in an attempt to make the Tl analogue of a known AM compound $\text{K}_2\text{Cu}_2\text{P}_4\text{Se}_{10}$.²⁷ Orange platelike crystals of $\text{Tl}_2\text{Cu}_2\text{P}_2\text{Se}_6$ were discovered in the reaction product. This compound has no known AM analogue and crystallizes in the monoclinic space group $P2_1/n$. The structure is shown in Figure 10 and consists of layers which cut diagonally through the ac plane and contain the b -axis. The layers are made up of P_2Se_6 units and trigonal planar CuSe_3 units. The Tl atoms are located near the surfaces of the sheets and have one-sided, 7-fold, coordination, suggesting active lone pairs protruding into the space between the layers (vide infra). Since $\text{Tl}_2\text{Cu}_2\text{P}_2\text{Se}_6$ forms orange crystals, its thermoelectric properties were not investigated.

$\text{Tl}_2\text{Au}_2\text{P}_2\text{Se}_6$. There are no AM compounds known that contain Au, P, and Se. This material was discovered during an investigation of the quaternary phase diagram. The elements were loaded in a 2:2:2:6 ratio and the reaction product contained black crystals in the form of irregular polyhedra. The crystals proved to be $\text{Tl}_2\text{Au}_2\text{P}_2\text{Se}_6$ which crystallizes in the monoclinic space group $P2_1/m$. The structure consists of 1-D chains along the c -axis and is presented in Figure 11. The chains are made up of $\text{Se}_3\text{P}-$

(26) Quint, R.; Boller, H. *Mater. Res. Bull.* **1987**, 22, 1499. Boller, H.; Klepp, K. O. *Mater. Res. Bull.* **1983**, 18, 437.

(27) Chondroudis, K.; Kanatzidis, M. G. *Inorg. Chem.* **1998**, 37, 2098.

(25) McCarthy, T. J.; Kanatzidis, M. G. *Chem. Mater.* **1993**, 5, 1061.

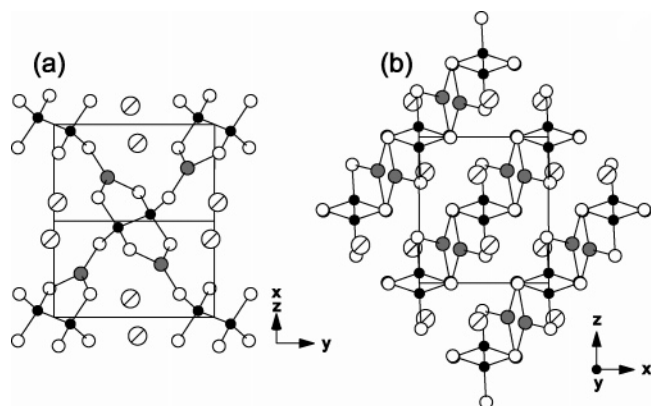


Figure 10. The crystal structure of $\text{Tl}_2\text{Cu}_2\text{P}_2\text{Se}_6$ viewed (a) perpendicular and (b) parallel to the layers showing Se atoms (white), P atoms (black), Cu atoms (gray), and Tl atoms (striped).

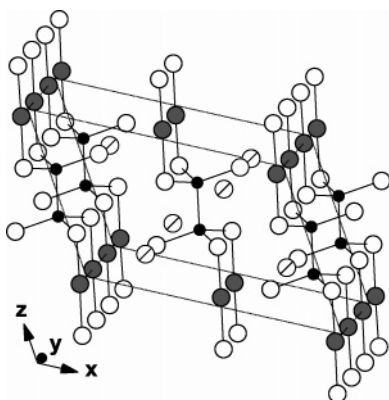


Figure 11. A view of the crystal structure of $\text{Tl}_2\text{Au}_2\text{P}_2\text{Se}_6$ showing Tl atoms (striped), P atoms (black), Au atoms (gray), and Se atoms (white).

PSe_3 units which are joined by two Au atoms in linear coordination to Se. Tl is irregularly coordinated to nine Se atoms (vide infra). Coordination environments and bond distances were used to distinguish between sites occupied by Tl (irregular, 9-fold) and Au (linear, 2-fold). Electron microprobe analysis was used to verify that both Tl and Au were present in the compound. Attempts to make this compound as a bulk sample produced the target compound as the majority phase ($\sim 90\%$) along with unidentified impurities.

$\text{TlInP}_2\text{Se}_6$. The elements were loaded in a 5:1:4:12 ratio in an attempt to make the Tl analogue of a known AM compound $\text{Cs}_5\text{InP}_4\text{Se}_{12}$.²⁸ Red needle-shaped crystals were discovered in the reaction product which proved to be $\text{TlInP}_2\text{Se}_6$. This compound has no AM analogue. The crystal structure is shown in Figure 12. $\text{TlInP}_2\text{Se}_6$ crystallizes in the triclinic space group $P\bar{1}$ and is composed of 1-D chains that run along the a -axis. The chains are made up of $\text{Se}_3\text{P}-\text{PSe}_3$ units and In in octahedral coordination to Se. The octahedra share edges and units bridge P_2Se_6 three different octahedral units. Tl atoms are between the chains and have irregular, 8-fold coordination (vide infra).

Since this compound is red, we did not investigate its thermoelectric properties.

$\text{Tl}_{11.5}\text{Sb}_{11.5}\text{Cu}_8\text{Se}_{27}$. This compound was discovered during an investigation of the quaternary phase diagram. The

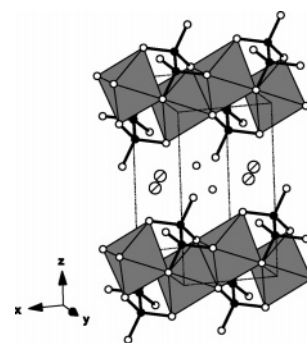


Figure 12. The crystal structure of $\text{TlInP}_2\text{Se}_6$ showing In-centered octahedra, P atoms (black), Se atoms (white), and Tl atoms (striped).

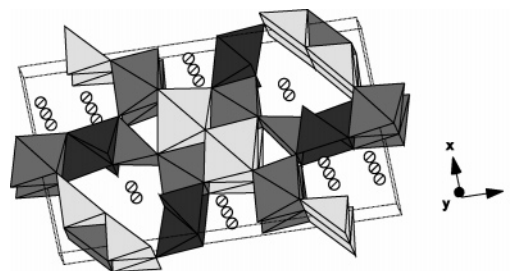


Figure 13. The crystal structure of $\text{Tl}_{11.5}\text{Sb}_{11.5}\text{Cu}_8\text{Se}_{27}$ showing Cu-centered tetrahedra (dark), Sb-centered polyhedra (medium), mixed Tl/Sb-centered polyhedra (light), and Tl atoms (striped).

elements were combined in a 2:2:2:5 ratio and the reaction product contained crystals of the title composition in the form of silver needles. $\text{Tl}_{11.5}\text{Sb}_{11.5}\text{Cu}_8\text{Se}_{27}$ is not isostructural to any known AM phase and crystallizes in the monoclinic space group $P2/m$. The crystal structure is shown in Figure 13 and includes Cu in tetrahedral coordination and Sb in both square pyramidal and octahedral coordination, common coordination environments for both elements. These polyhedra form a framework with channels running along the b direction in which the Tl atoms reside. Three of the Tl sites are partially occupied by Sb and are coordinated by Se in either square pyramidal or distorted octahedral geometry. Four are fully occupied by Tl and have 7-fold coordination by Se (vide infra). The ratio of Tl:Sb on one site is 1:3, and on the other two it is 3:1. This mixed occupancy balances the formal charges. Mixed occupancy of Tl and Sb is also seen in TlSbSe_2 , which has one site occupied equally by Tl and Sb, and Tl_9SbSe_6 , which has one site with 80% Tl and 20% Sb and another with 20% Tl and 80% Sb.^{29,30}

Pieces broken away from a single-phase ingot of this material were used for thermopower and resistivity measurements. The results of these measurements are shown in Figure 14 and indicate that $\text{Tl}_{11.5}\text{Sb}_{11.5}\text{Cu}_8\text{Se}_{27}$ is a p-type semiconductor.

Measured Band Gaps and Comparisons between Tl and AM Analogues. As pointed out in the Introduction, we expect the higher electronegativity of Tl to lead to lower band gaps and higher mobilities than found in isostructural AM compounds. Measured band gaps for eight of the compounds presented here are shown in Table 1, along with comparisons between Tl and AM analogues. Four of the AM materials for which we discovered Tl analogues have band

(28) Chondroudis, K.; Chakrabarty, D.; Axtell, E. A.; Kanatzidis, M. G. *Z. Anorg. Allg. Chem.* **1998**, 624, 975.

(29) Wacker, K.; Buck, P. *Mater. Res. Bull.* **1980**, 15, 1105.

(30) Gaeumann, A.; Bohac, P. *J. Less-Common Met.* **1973**, 31, 314.

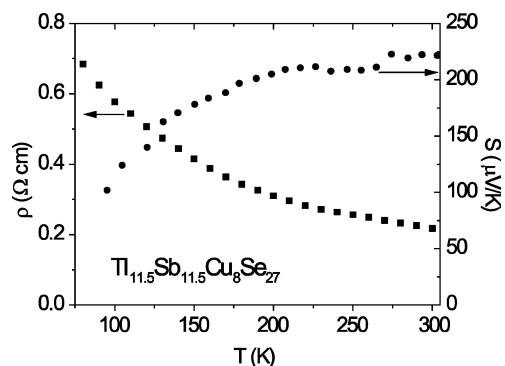


Figure 14. The measured thermopower (circles) and resistivity (squares) of $\text{Tl}_{11.5}\text{Sb}_{11.5}\text{Cu}_8\text{Se}_{27}$.

Table 1. Measured Band Gaps of Tl Compounds and Comparisons between Tl and AM Analogs

compound	color	E_{gap} (eV)
$\text{Tl}_2\text{Cu}_2\text{SnS}_4$	black	1.4
$\text{Rb}_2\text{Cu}_2\text{SnS}_4^{15}$	orange	2.08
$\text{Tl}_3\text{Ti}_2\text{P}_5\text{S}_{18}$	black-gold	1.3
$\text{K}_3\text{Ti}_2\text{P}_5\text{S}_{18}^{13}$	red-brown	1.61
$\text{Tl}_2\text{CeP}_2\text{S}_7^a$	yellow	2.4
$\text{K}_2\text{LaP}_2\text{S}_7^{12}$	colorless	> 3.5
$\text{Tl}_2\text{Au}_2\text{Sn}_2\text{Se}_6$	black	1.2
$\text{K}_2\text{Au}_2\text{Sn}_2\text{Se}_6^{23}$	red	2.28
$\text{Tl}_5\text{AgTi}_6\text{Se}_{27}^b$	black	$0.8(1.2 \times 10^4 \Omega\text{cm})$
$\text{Cs}_5\text{AgTi}_6\text{Se}_{27}^{16}$	black	$(2.5 \times 10^5 \Omega\text{cm})$
$\text{Tl}_3\text{CuNb}_2\text{Se}_{12}^c$	black	0.8
TlTiPS_5^d	black	1.3
$\text{Tl}_2\text{BiP}_2\text{S}_7^d$	red	1.8

^a We expect the Ce f electron to be localized and the replacement of La with Ce to have little influence on the band gap. ^b No band gap data are available for $\text{Cs}_5\text{AgTi}_6\text{Se}_{27}$. Resistivity at room temperature is compared in parentheses. ^c No data are available for AM analogue. ^d No isostructural AM analogue known.

gaps reported in the literature. In each case we found the Tl compound to have a smaller band gap than the AM compound. In the only case in which resistivity data is available for the AM compound, the Tl analogue was found to have a lower resistivity. These results are consistent with the expectation that the lower electronegativity of Tl should lead to improved electrical properties.

Tl Coordination Environments and Lone Pair Activity.

The coordination environments of the Tl atoms in all of the structures presented above are shown in Figure 15. For those compounds with several crystallographically distinct Tl sites, the coordination around each site is shown and labeled. If different sites have very similar environments, only one is shown. Brief descriptions of the environments are given in the discussions of individual compounds above. A table which lists the range of distances between Tl and S, Se, or Te that we consider to be a bond in each compound is included in the Supporting Information. It is important to note that often there is no obvious large gap in the Tl–chalcogen interatomic distance histogram to be used in defining the cutoff between those contacts considered to be bonds and those not considered to be bonds.

In Figure 15 Tl is seen to adopt a wide variety of coordination environments, from almost cubic to very irregular, with coordination numbers from five to ten. There are many instances in which the coordination is obviously

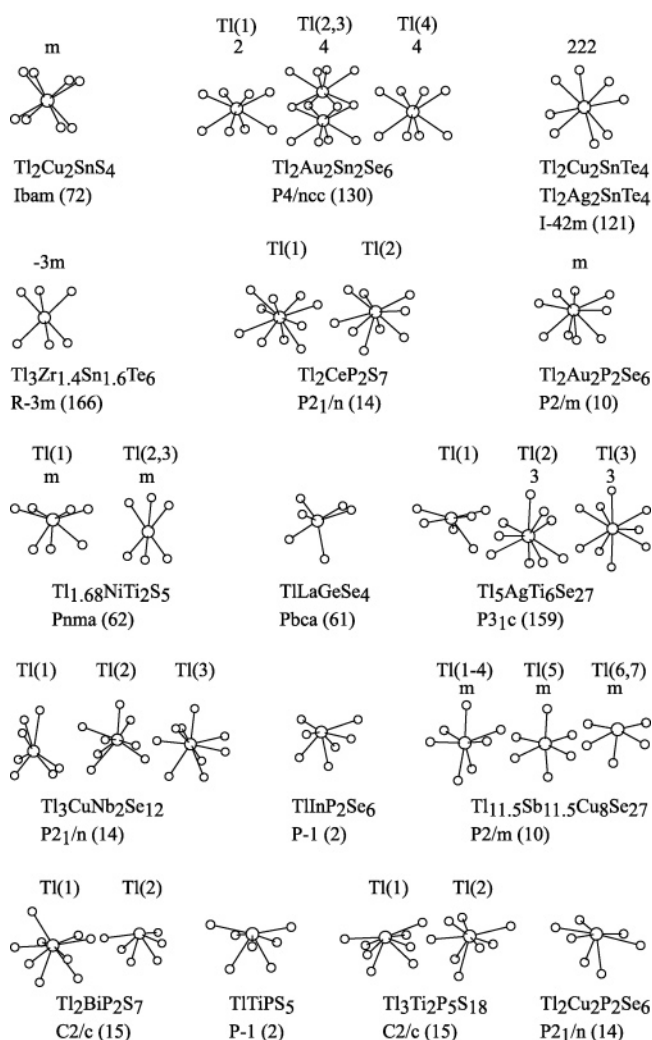


Figure 15. The coordination environments of Tl atoms in the compounds presented in this work. Each unit is labeled by the compound name and space group, and the site symmetry (if any) of the Tl site.

one-sided. This suggests that the lone pair on Tl in these situations is stereoactive and is protruding into the vacant part of the coordination environment. The compounds are loosely arranged from top to bottom based on the asymmetry of the arrangement of chalcogens around the Tl atom. Thus, the environments near the bottom of the figure are more likely to have active lone pairs than those at near top. We note that the most asymmetric environments tend to occur in the lower symmetry space groups.

Electron localization function (ELF) calculations³¹ were performed on two of these compounds, TlTiPS_5 and $\text{Tl}_2\text{-Cu}_2\text{P}_2\text{Se}_6$, and the results are shown in Figure 16. The plots show isosurfaces for $\eta = 0.855$. Also shown in Figure 16 is a ball-and-stick model of the structure oriented in the same way as in the ELF calculation. The ball-and-stick figure shows the coordination environment on the Tl atoms, and it is expected that the lone pair should point away from the coordinating chalcogens and into the empty part of the Tl coordination spheres. The figure shows electron density distributed around the chalcogen atoms, and also one-sided lobes of electron density on each Tl atom. These lobes

(31) Seshadri, R. *Proc. Indian Acad. Sci.* **2001**, *113*, 487.

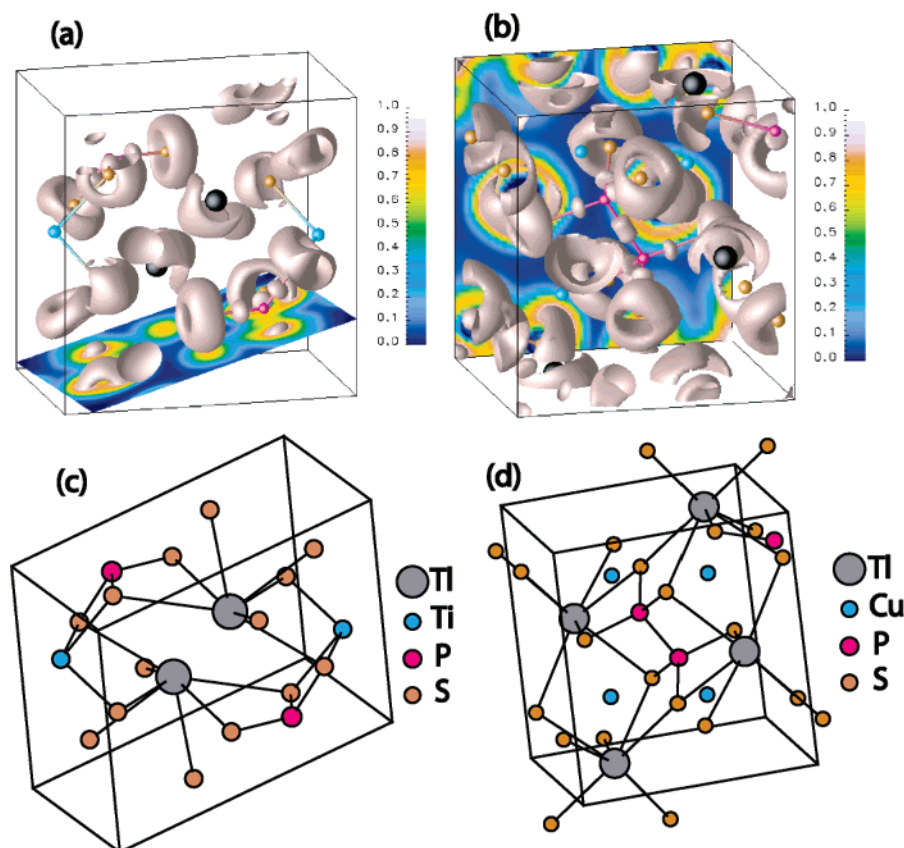


Figure 16. The results of ELF calculations for TlTiPS_5 (a) and $\text{Tl}_2\text{Cu}_2\text{P}_2\text{Se}_6$ (b). Ball-and-stick models oriented the same as the ELF figures are shown in (c) for TlTiPS_5 and (d) for $\text{Tl}_2\text{Cu}_2\text{P}_2\text{Se}_6$.

correspond to the lone pairs. Comparison of the ELF plot and the ball-and-stick model shows that the lone pairs indeed point into the gaps in the Tl coordination environments.

These results show that the lone pair of electron on Tl in chalcogenide compounds can be stereoactive. This is in contrast to AMs and may be partly responsible for the structural differences between Tl and AM compounds. In particular, TlTiPS_5 is similar but not isostructural to KTiPS_5 (vide supra). The coordination of Tl in TlTiPS_5 is more asymmetric than that of K in KTiPS_5 . This is due to a slight staggering of the $[\text{TiPS}_5]^-$ chains which opens a gap in the Tl coordination sphere. The ELF calculations (Figure 16) show that the lone pairs indeed reside in this gap.

Conclusions

We draw several conclusions from our initial investigation of quaternary thallium chalcogenide systems. First, it is clear that these are fertile grounds for new materials. This paper presents 17 new compounds with a wide variety of structural features and networks, from one- to three-dimensional. The synthesis and crystal structure determination of these compounds took place over only about 6 months, and according to the ICSD has increased the number of known quaternary Tl tellurides by a factor of 2 (from two to four), and the number of known quaternary Tl selenides by more than a factor of 3 (from three to eleven). There are many other Tl compounds that we have discovered but not yet studied, including sulfides, selenides, tellurides, and antimonides. The chemistry of Tl chalcogenides may be as rich as that of AM

chalcogenides. Some of the compounds presented here are isostructural to known AM compounds, but many are not. Perhaps the AM analogues of some of these new Tl compounds exist. We have shown evidence that the lone pair on Tl may influence the adopted crystal structure and may be responsible for some of the differences between Tl and AM compounds.

We have also seen evidence for some potential advantages of Tl chalcogenides over AM chalcogenides as TE materials. We have seen little evidence for sensitivity to air or moisture in these compounds (a few pressed pellets visibly tarnish in air after a few weeks). In every case in which a comparison can be made, the Tl compound was found to have a significantly smaller band gap or lower resistivity than the isostructural AM analogue (see Table 1). Some of the compounds were also shown to have extremely low thermal conductivity. There are no thermal conductivity data for isostructural alkali metal compounds with which to compare. However, it is very likely that the thermal conductivity of the Tl compounds will be lower than that of the AM compounds simply due to the larger mass of Tl. We have shown several examples of thermal conductivity less than half that of optimized Bi_2Te_3 alloys. These alloys typically have a thermal conductivity of 15 mW/cmK at room temperature, with a lattice contribution of approximately 10 mW/cmK.² It is possible that the low thermal conductivities seen for these Tl compounds can be further decreased through alloying between suitable compounds.

Despite these advantages, we have not yet found a material with promising TE properties. Most of the compounds do

show semiconducting behavior with low thermal conductivities, but the electrical resistivities are too large. It is possible that these materials can be doped to carrier concentrations that would improve their TE performance. We have made no attempt yet to study the doping behavior of these compounds. One challenge associated with complex, multinary compounds is doping without the formation of compensating defects. Our samples were not prepared with the ultra-high-purity starting materials and extreme care required to synthesize truly intrinsic samples, and yet the measured resistivities are high. This suggests that any unintentional doping is, in fact, being compensated. As prepared, none of the TI compounds that we have investigated to date can compete with the thermoelectric properties of Bi₂Te₃ alloys, or the AM compound CsBi₄Te₆.⁵ However, the number and diversity of potential new compounds seems large, and several ternary TI compounds have shown promise.^{8–10} This gives us hope that an advanced thermoelectric material will be found among TI chalcogenides.

Acknowledgment. This work was funded by NSF Grant # DMR-0011572. We thank Dr. Emil B. Lobkovsky for assistance in collecting single-crystal X-ray diffraction data and Prof. Ram Seshadri of the Materials Department at UCSB for performing the ELF calculations. We also thank John Hunt for guidance in using the electron microprobe facility in the Cornell Center for Materials Research which is supported through a MRSEC Grant (DMR-0079992). T.K.R. also thanks the American Society for Engineering Education for support through a National Defense Science and Engineering Graduate Fellowship (NDSEG).

Supporting Information Available: Experimental details regarding synthesis, characterization, and crystal structure refinement data (including CIF files). Figures showing structures of compounds that are isostructural to known AM compounds. ELF calculation details. Table regarding indexing of Tl₂Au₂Sn₂Se₆. Table of Tl–chalcogen bond distances. This material is available free of charge via the Internet at <http://pubs.acs.org>.

CM050412C